PHYSICAL REVIEW D VOLUME 20, NUMBER 9 1 NOVEMBER 1979

Electromagnetic radiative corrections to deep-inelastic neutrino interactions

Roger Barlow
Department of Nuclear Physics, University of Oxford, Oxford, England

Stephen Wolfram
Physics Department, California Institute of Technology, Pasadena, California 91125

(Received 1 December 1978)

The electromagnetic-radiative-correction factors to deep-inelastic neutrino-nucleon scattering are estimated using the parton-model formulas of Kiskis. Tables and approximate formulas are given for the benefit of experimenters wishing to estimate their own corrections. The corrections tend to be less than about 10%, and vary only slowly with energy, Q^2, and x.

I. INTRODUCTION

Experimental data on deep-inelastic lepton-nucleon scattering must be corrected for electromagnetic radiative effects before drawing conclusions about the behavior of strong interactions at short distances (scaling properties, structure functions, and so on). For charged-lepton–nucleon scattering the radiative corrections due to the lepton are routinely applied to data.[1] The corresponding calculation for neutrino-nucleon scattering is inevitably model-dependent, and this fact, combined with the relatively poor statistics of existing neutrino experiments, has led to the neglect of radiative corrections in this case. In the near future, experiments on neutrino scattering will yield more precise results, for which radiative corrections should not be neglected. In this paper we present a numerical study of these corrections based on the parton-model calculation of Kiskis.[2] Our results are not exact; they depend slightly on the details of the parton model used, and should only apply in the truly deep-inelastic region. We have evaluated the radiative-correction factors to a wide selection of differential cross sections for various energies and types of incoming neutrinos, chiefly muonic ones. They are typically around 5–10%, except in kinematic regions where the cross section is negligible.

II. THE MODEL

A. Charged-lepton scattering

The lowest-order diagram for charged-lepton–nucleon scattering is shown in Fig. 1. The lowest-order electromagnetic radiative corrections come from the diagrams of Figs. 2, 3, and 4 [diagrams not involving real photon emission contribute to the cross section at $O(\alpha^3)$ through interference with Fig. 1]. Self-energy diagrams for external lines are not drawn here or in later diagrams. If the cross section for Fig. 1 is known, the corrections due to the diagrams of Fig. 2 may be calculated in a model-independent manner; the processes depicted in Figs. 3 and 4 are usually ignored on the grounds that the lepton is more violently accelerated than the hadrons and, therefore, radiates more strongly. This assumption is undoubtedly valid for eN scattering; we discuss its validity for the μN case below. Since the graphs of Figs. 1 and 2 form a gauge-invariant set, their sum does not contain infrared divergences, though any individual diagram is of course in general infrared divergent.

The radiative process may be considered as having four effects:

(1) The outgoing particle's momentum may be altered, moving events from one kinematical configuration to another.

(2) The incoming particle's momentum may be altered, thereby changing the kinematic configuration for the event, and also the probability for the

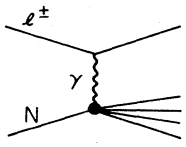

FIG. 1. The lowest-order diagram for charged-lepton–nucleon scattering.

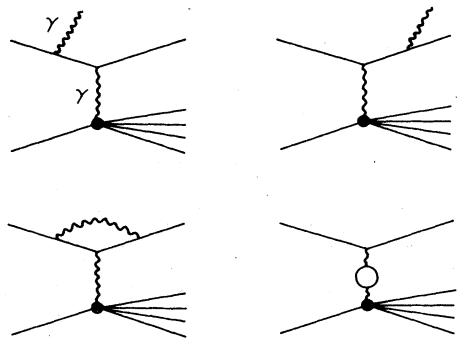

FIG. 2. First-order electromagnetic radiative corrections to Fig. 1: "leptonic" diagrams.

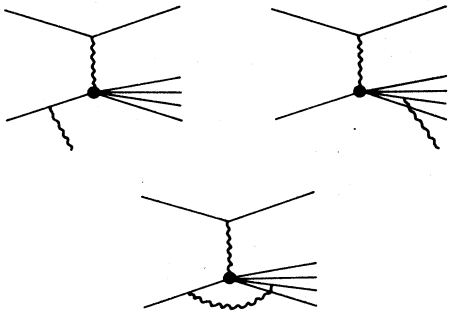

FIG. 3. First-order electromagnetic radiative corrections to Fig. 1: "hadronic" diagrams.

interaction (though the energy dependence of the cross section).

(3) The overall cross section for the process in a particular kinematical configuration will change.

(4) In experimental studies of exclusive processes, events may be discarded because particles radiate energy and momentum, so that the experimental energy-momentum constraints cannot be satisfied. If the energy-momentum lost in this way is small (and all particles will inevitably radiate to some extent), then the imbalance will not be noticed and the event will be accepted. The evaluation of this effect requires knowledge of the experimental acceptance, resolution, and fitting procedure. In practice all these details are combined into the energy resolution Δ of the experiment. (Δ may also be considered as the minimum detectable photon energy.) To lowest order these effects are typically proportional to $\log(E/\Delta)$. The effect (4) is not relevant for the inclusive processes that we discuss.

The evaluation of the diagrams for Figs. 3 and 4 would require a model for the hadron current. The parton model is an obvious possiblility. It has been used[3] to calculate $\sigma(l^+N)-\sigma(l^-N)$ due to two-photon-exchange diagrams. A more complete calculation has recently been done by Bardin and Shumeiko.[4] They find that the hadronic radiative corrections can be as large as -5%, but are always $<1\%$ in regions where the cross section is sizable. In addition one might except hadronic radiative corrections to give $\sigma(l^+N)\neq\sigma(l^-N)$. No such inequality has yet been observed,[5] in agreement with complete theoretical predictions.[4]

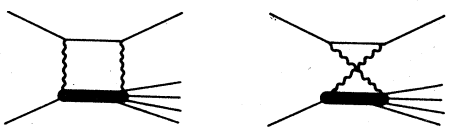

FIG. 4. First-order electromagnetic radiative corrections to Fig. 1: "two-photon exchange" diagrams.

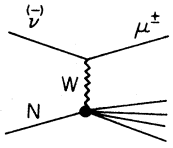

FIG. 5. The lowest-order diagram for charged-current νN scattering.

The parton model has proved adequate in explaining gross features of differential cross sections for deep-inelastic scattering, but it does not attempt to describe the evolution of the multihadron final state at large distances. It may, however, be photon interactions in this hadronic final state which form the main part of the hadronic electromagnetic radiative correction.

B. Neutrino scattering

The basic diagram for charged-current neutrino-nucleon scattering is shown in Fig. 5, and the lowest-order electromagnetic-radiative corrections to this process are given in Fig. 6 [diagrams in which photons couple to the W are typically suppressed by a factor $O(Q^2/M_W{}^2)$ and are consequently ignored]. Unlike the diagrams for charged-lepton scattering in Figs. 2, 3, and 4, those of Fig. 6 cannot be separated into gauge-invariant sets. They must therefore all be included in order to obtain an infrared-finite result. A model for the hadronic current is hence obligatory in these calculations. We use the parton model, and so the radiative-correction diagrams are those of Fig. 7. We take the W mass to be infinite (so that the weak interactions are pointlike), since the finiteness of its mass will not have appreciable effects at the energies we consider. The diagrams of Fig. 7 have been calculated in the deep-inelastic limit by Kiskis.[2] He finds that some of the radiative correction may be absorbed into renormalization of the weak coupling constant. The effective mass of

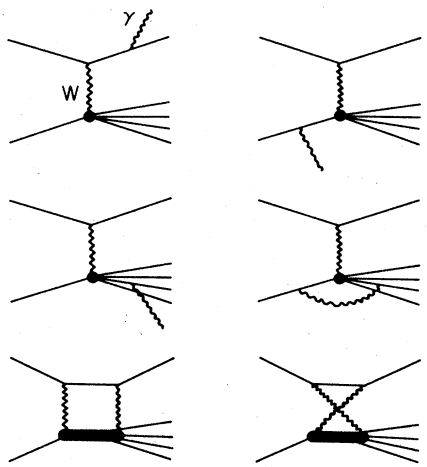

FIG. 6. First-order electromagnetic radiative corrections to Fig. 5.

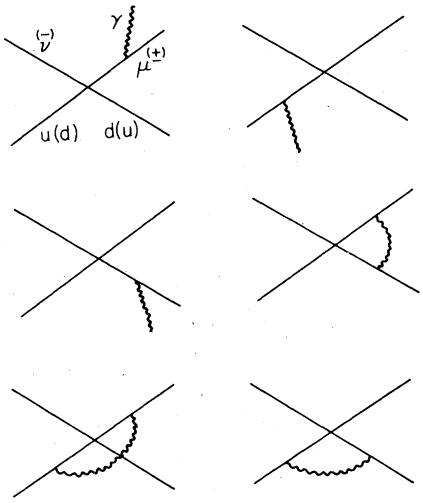

FIG. 7. Parton-model diagrams for electromagnetic radiative corrections to charged-current νN scattering.

the final parton is a free parameter (the mass of the initial parton is completely constrained by parton-model kinematics; if no photon is emitted it is approximately xM, where, as usual, $x = Q^2/2M\nu$), as is the initial parton $f(x)$ distribution. In Fig. 8 we show the correction factor by which theoretical predictions should be changed

$$\delta = (\sigma_{\text{corrected}} - \sigma_{\text{uncorrected}})/\sigma_{\text{uncorrected}}$$

as a function of x and y for various possible choices of the free parameters in the model, with an incoming antineutrino beam of energy 100 GeV. Figure 8(a) shows the corrections computed with the values of these free parameters as used in the rest of the paper (Field-Feynman quark distribution functions[6] and outgoing parton mass 0.3 GeV). Figures 8(b) and 8(c) are for outgoing parton masses of 0.001 and 0.9 GeV, respectively, and Fig. 8(d) shows the correction obtained using the quark distribution functions of Barger and Phillips.[7] Finally in Fig. 8(e) we show the results of using integer charged partons, although the success of the parton model essentially requires the partons to have the usual quark quantum numbers. These figures indicate that changes in the parameters in the model we use do not have any significant effect on our results.

It should be noted that the appearance of terms proportional to the logarithm of the parton mass is a simple consequence of the fact that it has been assumed that the momentum of the outgoing muon can be measured with arbitrary precision. If one allows for finite resolution in the detection of the muon, then the mass singularities disappear, and the logarithms of the parton mass are replaced by logarithms of the resolution.

III. RESULTS

We present numerical values for the radiative-correction factor

$$\delta = (\sigma_{\text{corrected}} - \sigma_{\text{uncorrected}})/\sigma_{\text{uncorrected}}$$

in the process $\nu N \to \mu X$ as a function of the kinematic variables x, y, and Q^2, defined by

$$Q^2 = -(p - p')^2, \quad y = (E - E')/E, \quad x = Q^2/2MEy, \tag{1}$$

where E, E', p, and p' are the energies and four-momenta of the incoming neutrino and outgoing muon, respectively.

Figure 9 shows the correction to $d\sigma/dy$ as a function of y with $E = 100$ and 500 GeV. Note that the model should not apply in regions where the outgoing muon or parton has small momentum; for this case these regions are y near 0 or 1. (A cut in Q^2 to avoid the elastic region has no important effects.) The general shape of the curves in Fig. 9 may be understood intuitively; the muon loses energy through bremsstrahlung, shifting events to higher y values. In Figs. 10, 11, and 12 we show corrections to various double-differential cross sections, as a function of y (Fig. 10) and Q^2 (Fig. 11) for various values of x, and as a function of x for various values of Q^2 (Fig. 12). The model should not be valid for small Q^2.

The dependence of δ on x at a given Q^2 (Fig. 12) appears to be approximately linear. We have accordingly fitted straight lines to the results, of the form $\delta = A + Bx$, and the values of A and B, for various Q^2 and E for neutrinos and antineutrinos, are tabulated in Table I. A simpler but adequate fit to all our results is given by the following: For neutrinos

$$\delta = -0.0375 - 0.000\,20E + 0.0266 \ln Q^2 - 0.214x,$$

and for antineutrinos

$$\delta = -0.0135 - 0.000\,20E + 0.0271 \ln Q^2 - 0.230x,$$

where E and Q are in GeV. The rms difference between the value of δ according to the fit and the value as computed is around 0.01, i.e., 1% of the uncorrected cross section.

Figure 13 shows the correction as a function of y for the process $\nu N \to eX$. These radiative corrections are rather larger than those with final muons (see Fig. 9) and will therefore add further to the difficulties of high-energy $\nu_e N$ experiments.

We have also calculated the radiative correction for the neutral-current process $\nu N \to \nu X$: It is negative, but smaller than 0.02 for $y < 0.7$.

IV. DISCUSSION

One of the principal aims of recent deep-inelastic neutrino experiments has been to investigate the

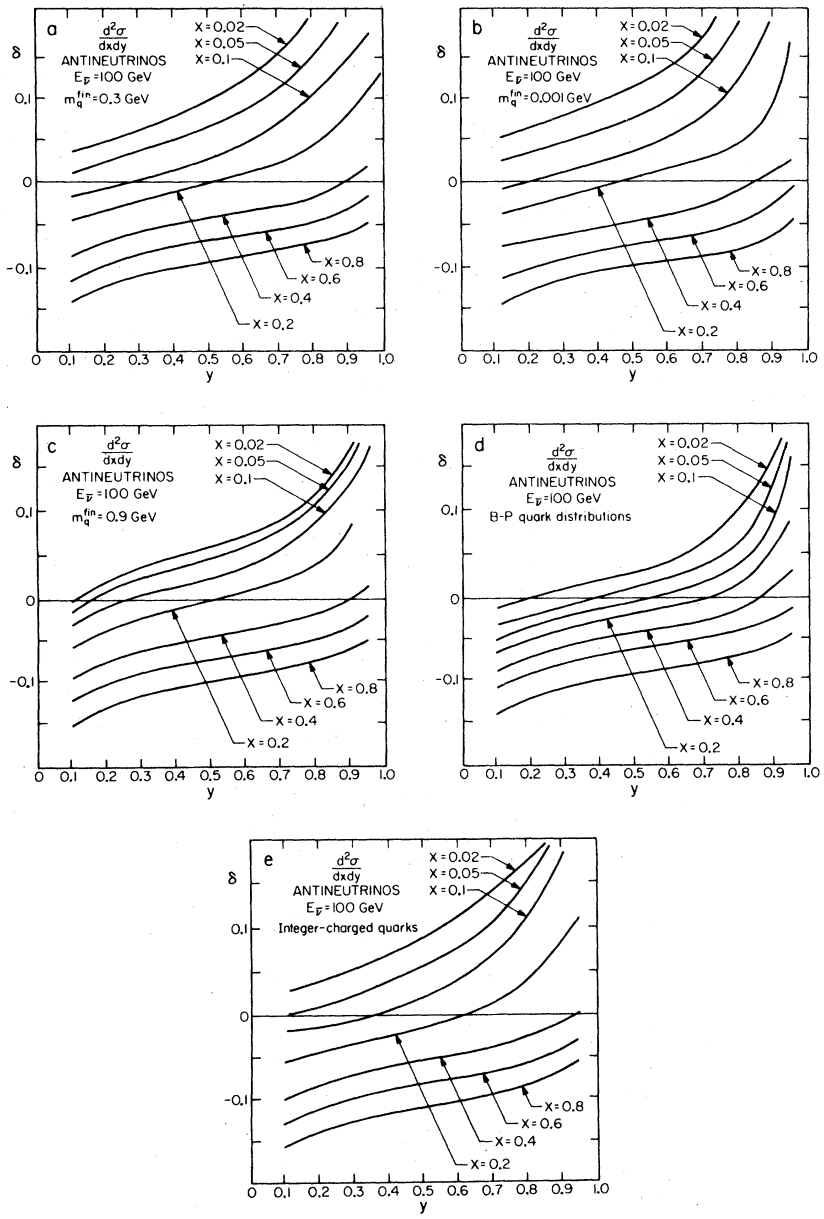

FIG. 8. The radiative-correction factors for $\bar{\nu}N$ deep-inelastic scattering with an incoming neutrino energy of 100 GeV for various choices of the free parameters in the model. (a) Outgoing parton mass = 0.3 GeV; Field-Feynman quark distribution functions (standard set of parameters). (b) Outgoing parton mass = 0.001 GeV; Field-Feynman quark distribution functions. (c) Outgoing parton mass = 0.9 GeV; Field-Feynman quark distribution functions. (d) Outgoing parton mass = 0.3 GeV; Barger-Phillips quark distribution functions. (e) Outgoing parton mass = 0.3 GeV; Field-Feynman quark distribution functions; integer-charged quarks.

violations of Bjorken scaling due to the nonscaling behavior of the strong interactions at short distances (strong radiative corrections). In Fig. 14 we show the corrections induced by these effects according to quantum chromodynamics (QCD), with standard input parameters.[8] They are typically somewhat larger than the electromagnetic radiative corrections presented above, but it is evident that the latter must be considered in a detailed comparison of experimental results with theoretical predictions. Strong interactions affect only the hadronic vertex, but electromagnetic ones affect both

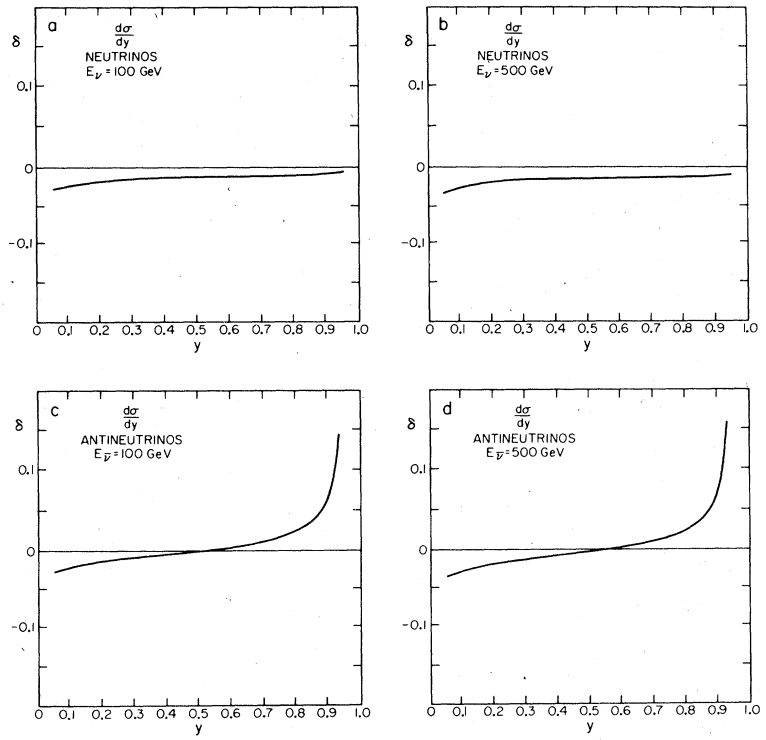

FIG. 9. Radiative-correction factors for $d\sigma/dy$. (Note that the model is inapplicable near $y=1$.)

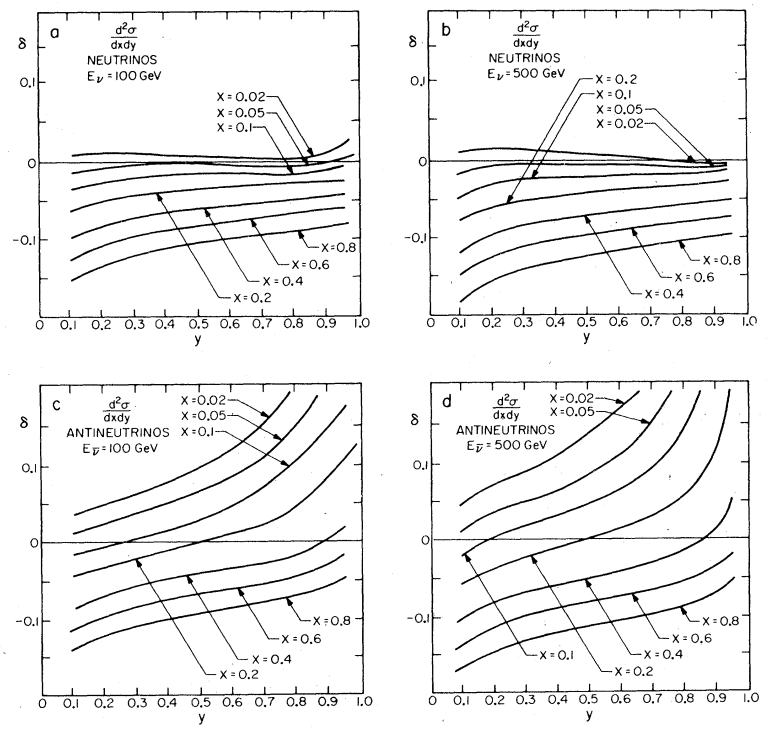

FIG. 10. Radiative-correction factors for $d\sigma/dx\,dy$.

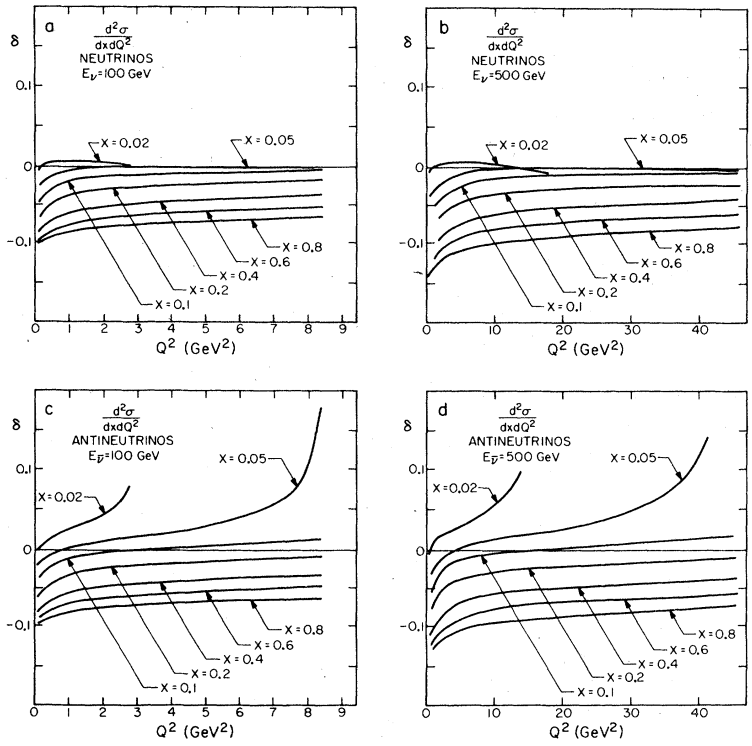

FIG. 11. Radiative-correction factors for $d\sigma/dx\,dQ^2$ as a function of Q^2 for various x.

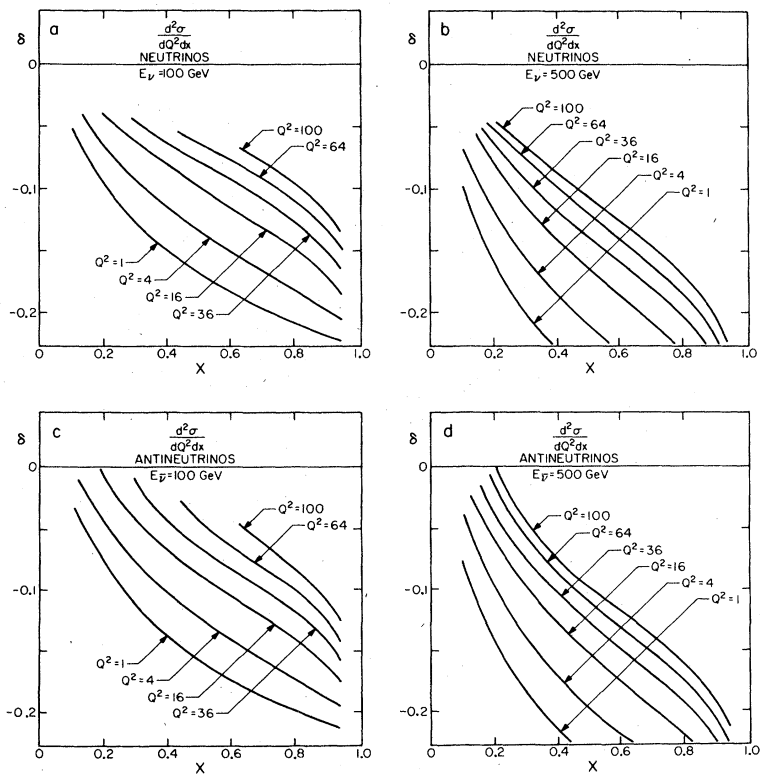

FIG. 12. Radiative-correction factors for $d\sigma/dQ^2\,dx$ as a function of x for various Q^2. Note the approximate linearity of the curves.

TABLE I. Linear fits to the correction factor of the form $\delta = A + Bx$.

Energy (GeV)	Q^2 (GeV^2)	Neutrinos A	Neutrinos B	Antineutrinos A	Antineutrinos B
50.0	1	−0.044	−0.166	−0.027	−0.173
	4	−0.016	−0.170	0.005	−0.183
	9	−0.003	−0.164	0.022	−0.183
	16	0.006	−0.158	0.033	−0.179
	25	0.017	−0.159	0.045	−0.179
	36	0.029	−0.161	0.060	−0.183
	49	0.056	−0.184	0.086	−0.202
	64	0.113	−0.237	0.151	−0.259
	81	0.321	−0.451	0.340	−0.438
100.0	1	−0.061	−0.189	−0.044	−0.196
	4	−0.027	−0.197	−0.008	−0.208
	9	−0.010	−0.195	0.011	−0.208
	16	−0.002	−0.186	0.023	−0.206
	25	0.004	−0.179	0.033	−0.204
	36	0.011	−0.174	0.040	−0.199
	49	0.019	−0.175	0.052	−0.202
	64	0.029	−0.177	0.061	−0.203
	81	0.046	−0.189	0.078	−0.213
	100	0.066	−0.205	0.103	−0.232
150.0	1	−0.073	−0.202	−0.056	−0.209
	4	−0.034	−0.215	−0.016	−0.223
	9	−0.017	−0.211	0.004	−0.225
	16	−0.010	−0.201	0.016	−0.221
	25	−0.000	−0.196	0.026	−0.218
	36	0.005	−0.190	0.034	−0.215
	49	0.013	−0.188	0.042	−0.213
	64	0.016	−0.183	0.049	−0.211
	81	0.020	−0.179	0.056	−0.212
	100	0.032	−0.186	0.067	−0.216
200.0	1	−0.083	−0.211	−0.064	−0.219
	4	−0.042	−0.225	−0.023	−0.235
	9	−0.022	−0.224	−0.001	−0.237
	16	−0.010	−0.218	0.011	−0.233
	25	−0.003	−0.211	0.021	−0.229
	36	0.002	−0.202	0.029	−0.226
	49	0.006	−0.196	0.035	−0.222
	64	0.011	−0.192	0.042	−0.220
	81	0.014	−0.187	0.047	−0.218
	100	0.022	−0.190	0.056	−0.219
250.0	1	−0.090	−0.218	−0.072	−0.226
	4	−0.048	−0.233	−0.028	−0.244
	9	−0.027	−0.233	−0.006	−0.246
	16	−0.016	−0.225	0.008	−0.243
	25	−0.007	−0.219	0.017	−0.238
	36	−0.001	−0.213	0.025	−0.234
	49	0.004	−0.207	0.032	−0.231
	64	0.007	−0.201	0.039	−0.230
	81	0.013	−0.198	0.042	−0.225
	100	0.014	−0.192	0.050	−0.226
300.0	1	−0.097	−0.224	−0.078	−0.232
	4	−0.052	−0.241	−0.033	−0.250
	9	−0.030	−0.241	−0.011	−0.251
	16	−0.018	−0.235	0.005	−0.252
	25	−0.010	−0.228	0.013	−0.245
	36	−0.005	−0.219	0.022	−0.243
	49	−0.001	−0.212	0.028	−0.238
	64	0.005	−0.209	0.034	−0.235
	81	0.007	−0.201	0.039	−0.231
	100	0.013	−0.202	0.045	−0.230

TABLE I. (*Continued*)

Energy (GeV)	Q^2 (GeV^2)	Neutrinos A	Neutrinos B	Antineutrinos A	Antineutrinos B
350.0	1	−0.102	−0.229	−0.083	−0.237
	4	−0.056	−0.247	−0.037	−0.256
	9	−0.035	−0.247	−0.014	−0.259
	16	−0.022	−0.240	0.000	−0.256
	25	−0.013	−0.235	0.011	−0.253
	36	−0.008	−0.225	0.019	−0.249
	49	−0.003	−0.219	0.026	−0.245
	64	0.006	−0.219	0.031	−0.241
	81	0.005	−0.209	0.038	−0.240
	100	0.009	−0.205	0.043	−0.238
400.0	1	−0.107	−0.233	−0.088	−0.241
	4	−0.061	−0.252	−0.041	−0.261
	9	−0.037	−0.254	−0.017	−0.263
	16	−0.024	−0.246	−0.002	−0.262
	25	−0.016	−0.239	0.010	−0.260
	36	−0.010	−0.231	0.016	−0.253
	49	−0.003	−0.228	0.024	−0.251
	64	0.000	−0.221	0.029	−0.246
	81	0.005	−0.217	0.035	−0.244
	100	0.007	−0.211	0.040	−0.243
450.0	1	−0.112	−0.237	−0.092	−0.245
	4	−0.063	−0.258	−0.044	−0.266
	9	−0.040	−0.258	−0.021	−0.268
	16	−0.026	−0.254	−0.006	−0.265
	25	−0.017	−0.246	0.005	−0.263
	36	−0.012	−0.237	0.015	−0.261
	49	−0.004	−0.233	0.020	−0.255
	64	−0.002	−0.225	0.027	−0.252
	81	0.003	−0.221	0.033	−0.250
	100	0.006	−0.217	0.036	−0.245
500.0	1	−0.116	−0.240	−0.096	−0.249
	4	−0.066	−0.262	−0.047	−0.269
	9	−0.042	−0.263	−0.023	−0.273
	16	−0.028	−0.258	−0.007	−0.271
	25	−0.019	−0.251	0.004	−0.268
	36	−0.014	−0.241	0.012	−0.263
	49	−0.009	−0.235	0.019	−0.260
	64	−0.004	−0.230	0.025	−0.256
	81	−0.000	−0.224	0.031	−0.254
	100	0.004	−0.220	0.035	−0.251

hadronic and leptonic vertices, so that while strong-interaction corrections depend only on x and Q^2/μ^2, electromagnetic corrections also depend on the incoming energy E. The dependence is slight except at large x, but it could perhaps be used to distinguish strong and electromagnetic scaling violations.

The typical magnitude of the electromagnetic radiative corrections to neutrino scattering found in this paper indicates that these effects should not be of great importance for previously published results, but must be considered in the next generation of experiments.

It should be emphasized again that our parton-model calculations are valid only in the kinematic region where all outgoing particles are relativistic, and also take no account of electromagnetic

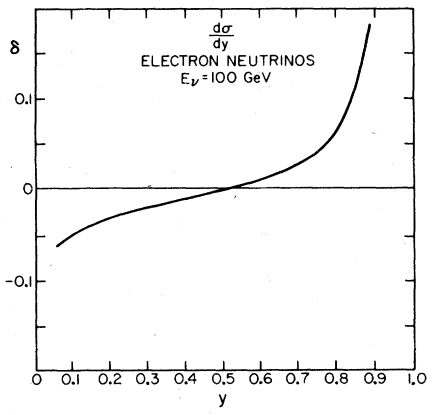

FIG. 13. Radiative-correction factor for $d\sigma/dy$ in $\nu_e N$ scattering.

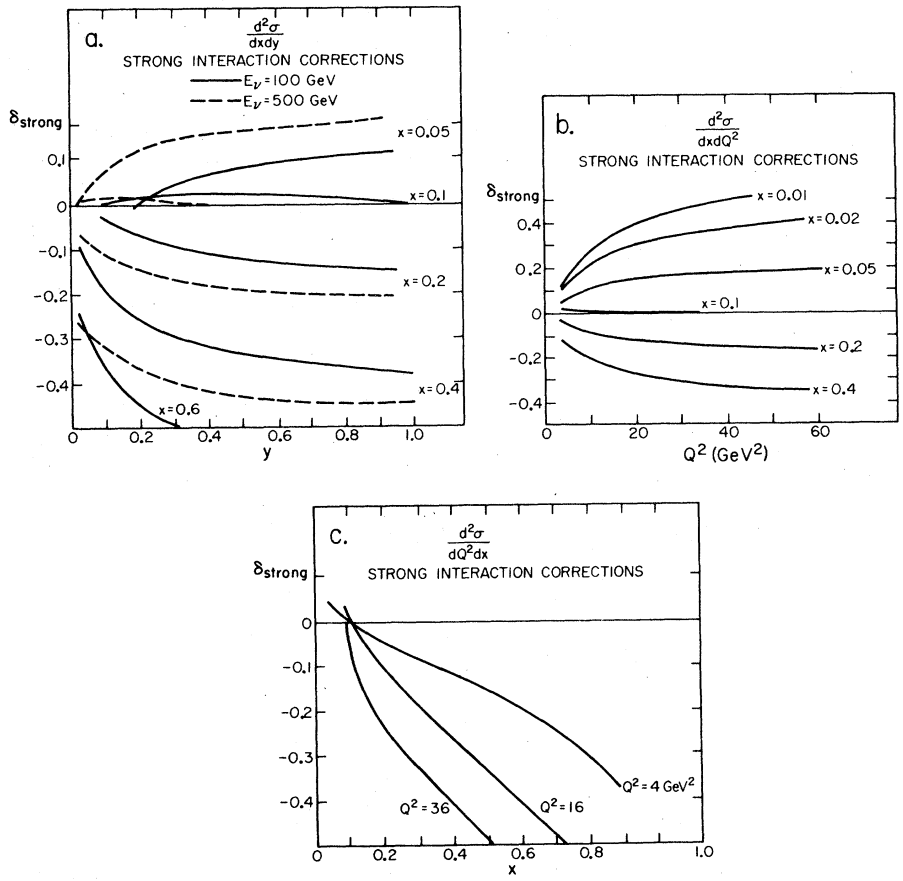

Fig. 14. Typical QCD corrections to various double-differential cross sections for νN scattering.

effects in the multihadron final state. Our results should therefore be treated only as estimates, rather than exact values for electromagnetic radiative corrections.

ACKNOWLEDGMENTS

We are grateful to C. Llewellyn Smith, D. Perkins, T. Quirk, and P. Schreiner for their interest in this work.

[1]L. W. Mo and Y. S. Tsai, Rev. Mod. Phys. 41, 205 (1969).
[2]J. Kiskis, Phys. Rev. D 8, 2129 (1973).
[3]J. Bartels, Nucl. Phys. B82, 172 (1974); P. M. Fishbane and R. L. Kingsley, Phys. Rev. D 8, 3074 (1973).
[4]D. Yu. Bardin and N. M. Shumeiko, JINR Report No. P2-10872 (unpublished).
[5]L. S. Rochester *et al.*, Phys. Rev. Lett. 36, 1284 (1976).
[6]R. D. Field and R. P. Feynman, Phys. Rev. D 15, 2590 (1977).
[7]V. Barger and R. J. N. Phillips, Nucl. Phys. B73, 269 (1974).
[8]A. J. Buras and K. J. F. Gaemers, Nucl. Phys. B132, 249 (1978).